JOURNAL OF MATERIALS SCIENCE 23 (1988) 879–885

Rate effects on the compression and recovery of dimensions of cork

M. EMÍLIA ROSA, M. A. FORTES
Departamento de Engenharia de Materiais, Instituto Superior Técnico, Instituto de Ciência e Tecnologia dos Materiais, Av. Rovisco Pais, 1096 Lisboa Codex, Portugal

A study of the effect of strain rate on the compression behaviour of cork was carried out, which takes into account the anisotropy of the material. Compression curves at three different rates were obtained for each of the three directions in cork (radial, axial and tangential). Strain-rate sensitivity coefficients, m, were also measured in experiments where the strain rate was suddenly changed during the tests. The values of m are fairly isotropic, around 0.06. For a given strain rate, the radial direction is stronger (i.e. larger stresses) than the other two, but these are not equivalent, the axial direction being slightly stronger for most of the strain interval between 0 and 80%. The recovery of dimensions following compression in each direction was also studied. The change in the three dimensions with time was monitored, following compression to 30% and to 80% strain in a given direction. In the first case, recovery is almost total after ~20 days, but for 80% compression the deformation is not completely recovered after unloading. The recovery rate decreases appreciably with time and increases with the degree of deformation previously imposed. An equation is proposed that describes the recovery behaviour with a reasonable accuracy.

1. Introduction

The elastic properties and the behaviour of cork in compression were characterized in an extensive study of the structure and mechanical properties of cork, published by Gibson *et al.* [1]. To a first approximation, cork is an elastically orthotropic material with axial symmetry in relation to the radial direction of the tree, implying that it has five independent elastic constants. The axial symmetry results from the fact that the cells in cork are (rectangular) prismatic, with the axes of the prisms along the radial direction. The average dimension of the cells in directions perpendicular to the radial direction is independent of direction, at least approximately. This and the fact that the pores (lenticular channels), which always occur in cork, are oriented in the radial direction, determine the axial symmetry about this direction.

The prismatic cells are packed in (radial) columns with their bases staggered. Cork is a cellular material with closed cells. The average number of lateral faces of the prisms is six (hexagonal prisms), and the average coordination number of the cells is ~14 [2, 3] (i.e. a cell has, on average, ~14 cells adjacent to it through faces).

The following nomenclature for the directions will be adopted: the radial direction is along the radius of the tree and is therefore parallel to the axes of the prismatic cells; the axial direction is the vertical direction in the tree; the tangential direction is perpendicular to the other two, and therefore tangent to the circumference of the tree. These three directions will be termed *principal directions*. The term *non-radial directions* is used to indicate the two principal directions perpendicular to the radial direction.

The cell walls in cork (lateral and basal faces of the prisms) are non-planar (Fig. 1). The lateral faces show undulations [1, 3], which have repercussions on the mechanical properties. The cells are smaller than in most man-made cellular materials, but their dimensions, including the thickness, may vary considerably from sample to sample, and even from point to point in a given sample, especially along the radial direction. This is due to the fact that the size of the cells depends on the season when they were generated by the parenchymal tissue in the periphery of the bark. Typical dimensions are as follows: height of the cells, 40 μm; width of lateral faces, 20 μm; wall thickness, 2 μm. The number of cells per unit volume is typically 3.5×10^7 cm^{-3}. On the other hand, large variations are also found in the number and size of pores and other defects. The quality of cork is closely related to the volume fraction of pores that it contains. These large variations in structure are reflected in an appreciable scatter in the measured properties, with the corresponding difficulty of obtaining reliable data for cork.

Gibson *et al.* [1] obtained compression curves for cork, for each of the three principal directions. They found that the curves for compression parallel to the axial and tangential directions were nearly coincident, but that the curve for radial compression was well above the other two, implying a larger Young's modulus, E, along this direction. The reported values of E are 20 MPa in the radial direction and 13 MPa in the non-radial directions. They also measured the

0022–2461/88 $03.00 + .12

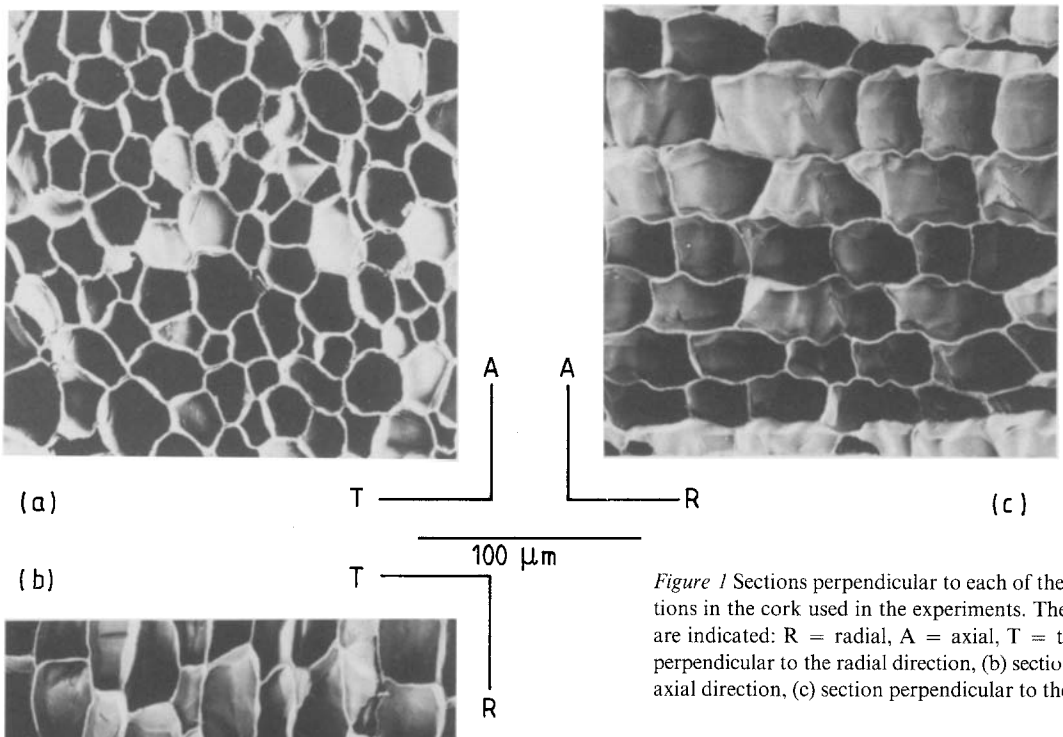

Figure 1 Sections perpendicular to each of the three principal directions in the cork used in the experiments. The other two directions are indicated: R = radial, A = axial, T = tangential. (a) Section perpendicular to the radial direction, (b) section perpendicular to the axial direction, (c) section perpendicular to the tangential direction.

Poisson ratios, ν, and found that for radial compression $\nu \simeq 0$, while $\nu \simeq 0.5$ for compression in the non-radial directions.

The compression curves always show three distinct regions to which can be assigned different deformation mechanisms [1]. These three regions are in fact found in the compression of any flexible foam [4]. The first, low-strain region, is "elastic" and corresponds to the reversible bending of the cell walls. The elasticity is non-linear, however, and this raises difficulties in the measurement of a characteristic modulus. As will be shown in the present study, the viscous component of deformation cannot be neglected and probably contributes to the non-linearity of the elastic regime. When a critical stress is reached, the cell walls start to buckle, in a cooperative fashion, and the slope of the compression curve decreases. Finally, when the buckling is general and the cell walls start to contact each other, the porosity is reduced and the slope again increases, eventually approaching the Young's modulus of the cell wall material.

This model for the compression of cellular materials was developed by Gibson and co-workers [5, 6], who also obtained equations relating various properties measured in compression to the density of the cellular material and to properties of the cell wall material. The model is quite satisfactory for cork, in spite of the fact that it does not include the effect of pores and the viscous component of deformation.

Our aim in this paper is to report on various viscous effects on the deformation of cork. Special attention will be given to strain-rate effects on the compression of cork and to the recovery of linear dimensions upon unloading. Related phenomena, namely the stress relaxation and creep behaviour of cork, will be reported in a companion paper [7].

The viscoelastic properties of cork and other cellular materials are, of course, quite important in their applications. For example, in the main application of cork in bottle stoppers, cork is strongly and rapidly compressed when introduced for the first time in the bottle and then stress-relaxes. When the stopper is removed, the dimensions partly recover; when it is re-introduced in the bottle a new cycle starts. In floor tiles, cork may be submitted to creep loadings, and its deformed shape will recover, perhaps not fully, after unloading. Finally, in the manufacture of cork products, the material is often deformed at high rates; virtually nothing is known on the strain-rate sensitivity of cork. The paper will address some of these questions.

We shall not be concerned with the variation in properties measured in samples taken from different places in the same tree or from different trees, although this is an important topic in relation to cork quality. The study will concentrate on a single batch of good-quality cork, previously submitted to a boiling operation. This operation consists of immersing cork in boiling water for a period of about 1 h, followed by drying in open air, and is applied to all cork boards before any processing.

After characterizing the cork used in the experiments (Section 2), we indicate the experimental results on the effect of strain rate on the compression curves along each of the three principal directions, and the data on the kinetics of recovery following compression (Section 4). In Section 5 we attempt to rationalize the experimental results and propose a

simple empirical equation to describe the recovery data.

2. Characterization of the cork used in the experiments

Boiled cork from a single cork board of good quality (low porosity) was used. The number of pores per unit area (perpendicular to the radial direction) was $\sim(14 \pm 3)\,cm^{-2}$, with an average pore diameter of ~ 0.05 cm. Scanning microscopy was used to observe the cell structure (Fig. 1). The average number of cells per unit volume was found to be $\sim 6 \times 10^7\,cm^{-3}$. The average height of the prisms is $\sim 34\,\mu m$ and the side of the average hexagonal basis $\sim 14\,\mu m$. Finally, the thickness of the walls was very uniform with a value of $\sim 1.5\,\mu m$. As Figs 1b and c show, the lateral walls of the cells are corrugated with one to three undulations per face. The bases of the cells are also non-planar, but in general with no undulations.

The water content measured by the weight loss at 100° C was 7 wt %. The density was measured from the volume and weight, leading to an average density of $172 \pm 6\,kg\,m^{-3}$.

3. Experimental procedure

The samples for mechanical testing were cut in a special device in the form of cubes of 16 mm edge, with their faces perpendicular to each of the three main directions. The cubes were equilibrated in the laboratory atmosphere and then compressed in a testing machine at three different crosshead speeds (0.2, 2 and 20 mm min^{-1}). These correspond to (nominal) strain rates, $\dot{\varepsilon}$, of 2.1×10^{-4}, 2.1×10^{-3} and $2.1 \times 10^{-2}\,sec^{-1}$, obtained by dividing the crosshead speed by the initial length of the cube edges. Three tests were made for each speed and each direction. All samples were compressed up to a strain $\varepsilon = 0.8$ with ε defined as

$$\varepsilon = \frac{l_0 - l}{l_0} \qquad (1)$$

where l and l_0, are respectively, the current and initial dimensions parallel to the compression axis. In addition to recording the complete stress–strain curves (stress is obtained by dividing the compression load by the initial area, 16 mm × 16 mm), various values were automatically recorded: the Young's modulus, E, defined as the ratio between the increment of stress and the increment of strain from $\varepsilon = 0.010$ to $\varepsilon = 0.015$; and the stresses at various strains including the final strain (0.8). The cubes were removed from the machine and their dimensions were measured at once and subsequently at regular time intervals up to ~ 70 days.

Similar experiments at the strain rate of $2.1 \times 10^{-2}\,sec^{-1}$ were conducted up to a strain of 30% and the recovery of dimensions was measured in the same way. This strain is located in the second, plateau region of the stress–strain curve, while the 80% strain is in the final, large-slope region.

Finally, experiments were done in which the crosshead speed was suddenly changed, at a pre-chosen strain, while the compression curve was being recorded. The strain rates used in these "strain-rate cycling" experiments were the same as in the simple compression tests.

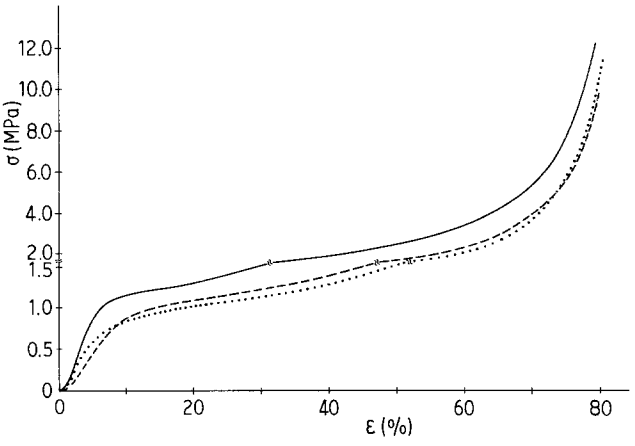

Figure 2 Typical stress–strain curves in compression along each of the principal directions: (——) radial, (– – –) axial, (· · ·) tangential. The curves are for $\dot{\varepsilon} = 2.1 \times 10^{-2}\,sec^{-1}$. There is a change of scale in the σ axis at $\sigma = 1.6$ MPa.

All experiments and measurements were done at room temperature (~20° C).

4. Results

As already noted, there is an appreciable scatter in the results even if the specimens are taken side by side from the same cork board, as was the case. When values of a property were measured in different specimens tested under the same conditions, the average values will be indicated together with the standard deviation. The compression curves shown are the more representative curves ("average" curves) for each set of conditions.

Fig. 2 shows stress–strain curves obtained at the crosshead speed of 20 mm min^{-1} ($\dot{\varepsilon} = 2.1 \times 10^{-2}\,sec^{-1}$) in compression along each of the three principal directions. The curves are of the type found by Gibson *et al.* [1], and, as these authors also noted, the curve for the radial direction is well above (larger stresses) the curves for the other two directions.

A new feature found in this study is that the curve for axial compression is definitely above the curve for tangential compression at the same strain rate. However, the two curves may cross at very low and very

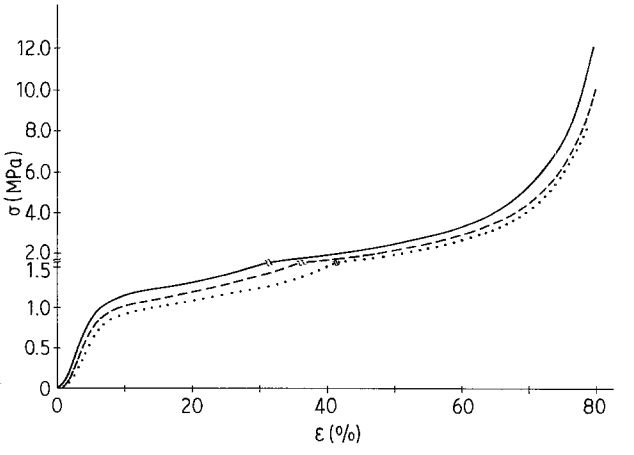

Figure 3 Effect of strain rate on the compression curve for the radial direction. There is a change of scale in the σ axis at $\sigma = 1.6$ MPa. Values of $\dot{\varepsilon}$ (sec^{-1}): (——) 2.1×10^{-2}, (– – –) 2.1×10^{-3}, (· · ·) 2.1×10^{-4}.

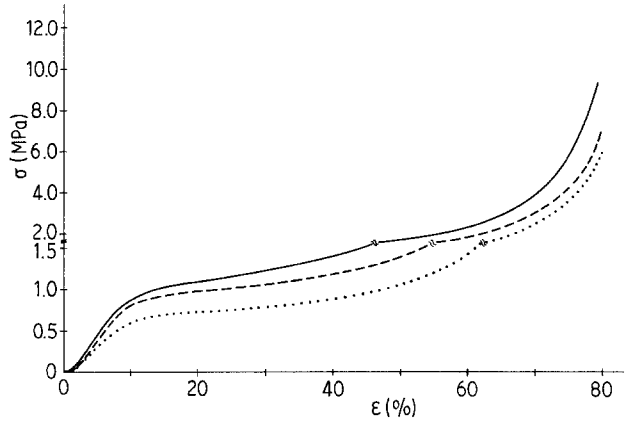

Figure 4 Effect of strain rate on the compression curve for the axial direction. There is a change of scale in the σ axis at σ = 1.6 MPa. Values of $\dot{\varepsilon}$ (sec^{-1}): (——) 2.1×10^{-2}, (– – –) 2.1×10^{-3}, (· · · ·) 2.1×10^{-4}.

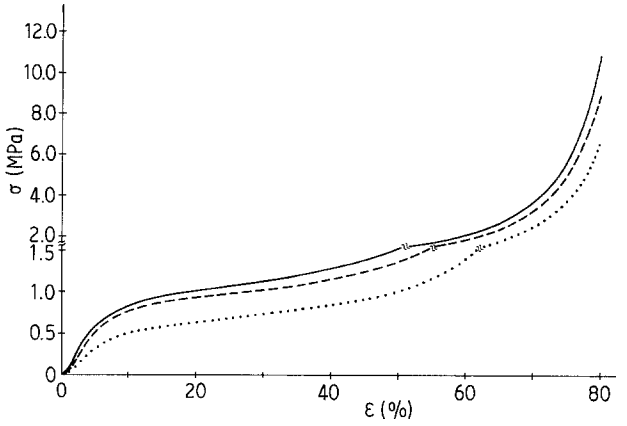

Figure 5 Effect of strain rate on the compression curve for the tangential direction. There is a change of scale in the σ axis at σ = 1.6 MPa. Values of $\dot{\varepsilon}$ (sec^{-1}): (——) 2.1×10^{-2}, (– – –) 2.1×10^{-3}, (· · · ·) 2.1×10^{-4}.

high strains, as in Fig. 2. This observation implies that the two non-radial directions are not equivalent. The reason for this must be found in a more detailed analysis of the structure of cork, including the cell structure and the pore structure. Another feature of the compression curves is the non-linearity of the first, or "elastic", region. In general the curves in this region are concave downwards, but quite often they show an inflection point, starting with the concavity upwards. As already pointed out, this raises difficulties in the definition of a Young's modulus.

We shall now describe separately the results related to the strain-rate effects in compression, and the results on recovery of dimensions following unloading.

4.1. Deformation rate effects

Figs 3 to 5 show stress–strain curves obtained in compression along each of the principal directions at each of the strain rates used in the experiments. All such tests were done up to 80% strain, when the dimension along the direction of compression had decreased from the initial value of 16 mm to 3.2 mm.

As expected, the stress increases as the rate increases, for each direction of compression. In Table I are indicated various quantities that show the rate effect. The values of Young's modulus, E, are the average slopes of the stress–strain curves between ε = 1% and ε = 1.5%. These values are considerably smaller than those reported by Gibson *et al.* [1]. In fact, the latter values are fairly close to the maximum slopes of the curves obtained in our experiments. The smaller values of E for the axial direction in Table I are related to the relative position of the curves in the elastic region, as discussed above. The other quantities listed in Table I are the stresses for strains of 10, 25 and 80%, respectively σ_{10}, σ_{25} and σ_{80}.

Each of the stresses σ_{10} and σ_{25} is, for the same $\dot{\varepsilon}$, larger for the radial direction and smaller for the tangential direction. However, the stress σ_{80} is smaller for the axial direction, which is associated with the crossing of the non-radial curves at large strains.

Table I also includes the energy per unit volume, W, spent in the deformation up to 80%. The values are nearly equal for the two non-radial directions. All energies increase with strain rate.

From Table I it is possible to obtain values for the strain-rate sensitivity coefficient, m, defined as

$$m = \frac{\mathrm{d}(\ln \sigma)}{\mathrm{d}(\ln \dot{\varepsilon})}$$

However, considering the scatter in the values of σ for a given strain and strain-rate, it is more accurate to obtain m from the measurement of the change in σ due to a sudden change in strain rate, using a single specimen for each determination of m. Fig. 6 shows a compression curve obtained under these conditions. The specimen was initially loaded at $2.1 \times 10^{-3}\ sec^{-1}$. At a strain of ~25%, the strain rate was changed to $2.1 \times 10^{-2}\ sec^{-1}$. Finally, at a strain of ~50% the strain rate was again changed to $2.1 \times 10^{-4}\ sec^{-1}$. A number of tests of this type were done to obtain, for each of the three principal directions, values of m at the strains of 5, 25, 50 and 75%. In Table II are indicated the values of m obtained in these experiments.

TABLE I Effect of strain rate on various properties of cork measured in compression tests

$\dot{\varepsilon}$ (sec^{-1})	Direction of compression	E (MPa)	σ_{10} (MPa)	σ_{25} (MPa)	σ_{80} (MPa)	$W \times 10^{-6}$ ($J\,m^{-3}$)
2.1×10^{-4}	Radial	6.0 ± 2.2	0.95 ± 0.04	1.20 ± 0.04	10.02 ± 1.71	1.83 ± 0.17
	Axial	3.1 ± 0.8	0.63 ± 0.09	0.79 ± 0.12	5.93 ± 0.89	1.07 ± 0.17
	Tangential	4.9 ± 0.8	0.54 ± 0.04	0.73 ± 0.05	6.81 ± 0.71	1.06 ± 0.08
2.1×10^{-3}	Radial	7.1 ± 1.5	1.00 ± 0.03	1.26 ± 0.03	9.76 ± 0.38	1.86 ± 0.04
	Axial	4.0 ± 2.3	0.82 ± 0.04	1.05 ± 0.09	8.19 ± 1.48	1.40 ± 0.17
	Tangential	8.5 ± 1.5	0.75 ± 0.06	0.97 ± 0.07	9.32 ± 0.90	1.41 ± 0.11
2.1×10^{-2}	Radial	13.0 ± 1.2	1.16 ± 0.07	1.43 ± 0.04	11.26 ± 0.87	2.05 ± 0.07
	Axial	6.0 ± 0.3	0.90 ± 0.03	1.18 ± 0.03	9.40 ± 0.16	1.56 ± 0.10
	Tangential	12.5 ± 1.0	0.85 ± 0.02	1.06 ± 0.02	10.85 ± 0.48	1.50 ± 0.05

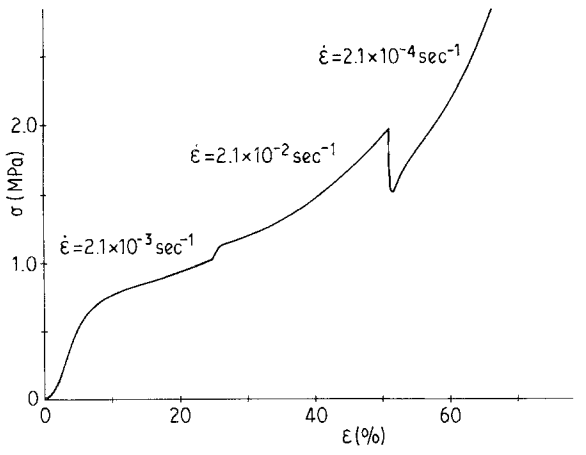

Figure 6 Strain-rate cycling experiment during radial compression.

They are of the same order as, although more accurate than, those that can be obtained by comparing the complete stress–strain curves at different rates. A slight tendency for m to increase with strain can be noted in Table II. Also to be noted is the fact that m is isotropic, within the accuracy of the measurements.

4.2. Recovery of dimensions

Let l denote the edge length at an instant t measured from the moment of unloading. The recovery will be indicated by $\varepsilon_r(t)$, defined as

$$\varepsilon_r = \frac{l - l_0}{l_0} \qquad (2)$$

where l_0 is the edge length before any compression ($l_0 \sim 16$ mm). ε_r is of course negative for the direction of compression and positive for the other two directions.

The first time that the dimensions were measured was taken to correspond to $t = 60$ sec, the average estimated time to accomplish the unloading and first length measurement.

Fig. 7 shows the recovery data for the extreme strain rates used, following compression to $\varepsilon = 80\%$. The experimental points are not indicated for the sake of clarity. These experiments were done in triplicate for each of the three directions and each of the three strain rates. Fig. 7 contains the measured values of $\varepsilon_r(t)$ for the three principal directions following compression at two different rates in each of the three principal directions. The absolute values of ε_r decrease in all cases but do not seem to tend to zero. (A cork stopper does not fully recover its initial dimensions even if it is left unloaded over a period of years.)

Similar experiments on the recovery of dimensions were done following compression to $\varepsilon = 30\%$, but only for the strain rate of $2.1 \times 10^{-2}\,sec^{-1}$. The corresponding curves are shown in Fig. 8. The dimensions are almost fully recovered after ~ 20 days ($|\varepsilon_r| < 1\%$ in the compression direction).

It is apparent from the results that the recovery curves $\varepsilon_r(t)$ for the direction of compression are, for a given strain rate, fairly independent of the direction of compression, although a slightly larger recovery seems to occur for the radial direction in the case of $\varepsilon = 0.8$ (but not for $\varepsilon = 0.3$). The recovery in the compressed direction is therefore fairly isotropic.

TABLE II Strain-rate sensitivity coefficient, m, of cork, measured at various strains

Direction of compression	m (5%)	m (25%)	m (50%)	m (75%)
Radial	0.04	0.05	0.05	0.07
Axial	0.05	0.06	0.06	0.07
Tangential	0.05	0.06	0.05	0.07

As regards the dimensions in directions perpendicular to the compression direction, the following observations are relevant. When the compression is radial, the strain in the tangential direction is larger than in the axial direction, again showing the non-equivalence of these two directions. For $\varepsilon = 80\%$ in the radial direction at $\dot{\varepsilon} = 2.1 \times 10^{-2}\,sec^{-1}$, the values of ε in the other two directions, measured 1 min after unloading, are as follows: axial direction $4.0 \pm 0.5\%$, tangential direction $6.3 \pm 1\%$. When the compression is tangential or axial, the smallest transversal strain always occurs in the radial direction, and is quite small ($\varepsilon = 2.0 \pm 0.6\%$ for 80% compression in the non-radial direction).

Finally, the recovery rate, measured by the absolute value of the slope of the $\varepsilon_r(t)$ curves, decreases with time and increases as the absolute value of the initial strain ($t = 0$) increases.

Regarding the effects of strain rate, it is first noted that there seems to be an increase of the transversal dimensions with increasing strain rate, for a constant compression strain. The recovery rate in the compression direction increases with strain rate. This tendency seems to decrease with time for compression in the radial direction, the opposite being observed for compression in the non-radial directions. The effect of strain rate in the recovery of the transversal dimensions is very small and no definite conclusions can be drawn.

5. Discussion

The strain-rate effects described in this paper show that the viscous component of deformation is quite important in the compression behaviour of cork. The strain-rate sensitivity coefficients are fairly large and so is the effect of rate on the energy spent in compression. The accuracy of the experiments was not sufficient to detect any anisotropy of the strain rate sensitivity coefficient, m. The values of m were, nevertheless, found to increase slightly with strain from 0.05 at low strains to 0.07 at large strains.

The compression behaviour indicates that the non-radial directions (i.e. the axial and the tangential directions) are not exactly equivalent, the axial direction being slightly more resistant, except, eventually, at very small and very large strains.

All this combined shows the complexity of the deformation of cork, and indicates the necessity of including the viscous component of deformation in a more refined model for the mechanical properties of cork.

The recovery of dimensions is a slow process but

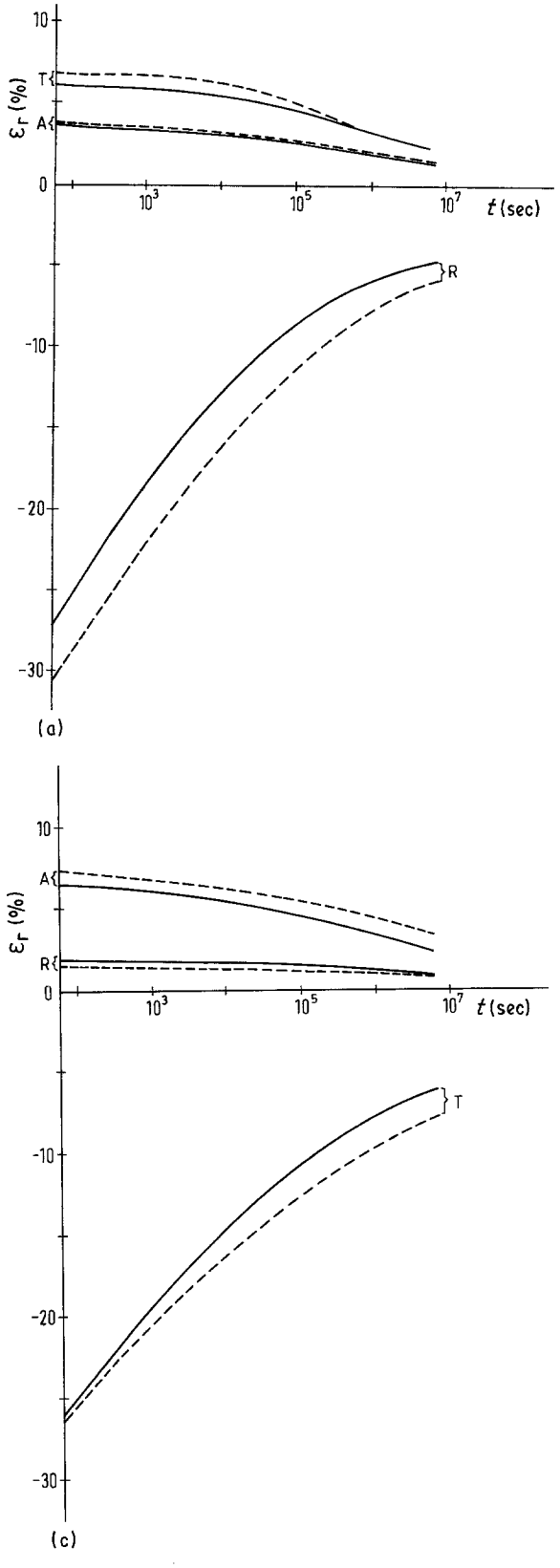

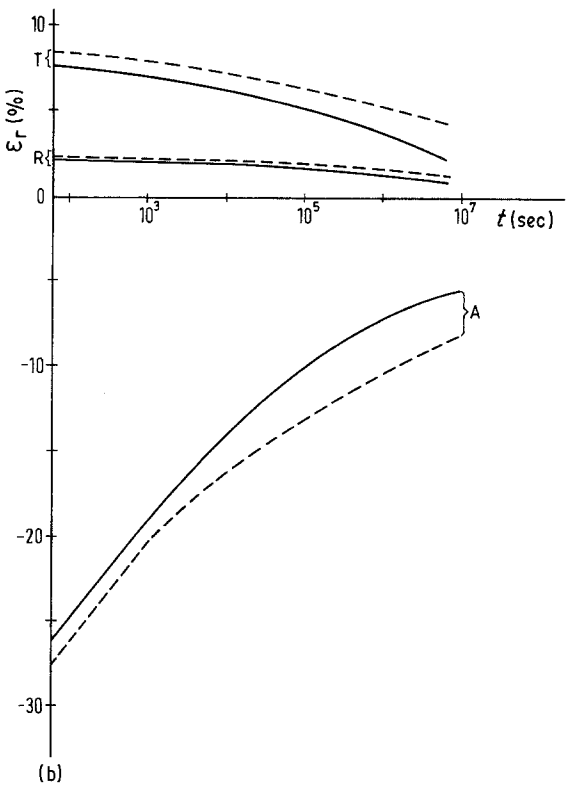

Figure 7 Recovery of dimensions of cork (R = radial dimension, A = axial dimension, T = tangential dimension) following compression up to $\varepsilon = 80\%$ at two strain rates, (– – –) 2.1×10^{-4} sec^{-1} and (——) 2.1×10^{-2} sec^{-1}. (a) Compression in the radial direction, (b) compression in the axial direction, (c) compression in the tangential direction.

practically full recovery is achieved after fairly low strains, e.g. $\varepsilon = 0.3$. Upon compression to very high strains, e.g. $\varepsilon = 0.8$, a permanent deformation remains even after ~ 70 days.

When cork is compressed above the threshold for initiation of cell wall buckling (i.e. above $\sim 10\%$ strain), subsequent recovery of dimensions is expected to be associated with the unfolding of the buckled cell walls, which, in turn, must involve relaxation processes at the molecular level, occurring in the cell walls. It is expected that before full recovery, cork will be less strong than in the undeformed or fully recovered states, since the corrugations will be more pronounced, implying a smaller stiffness of the cell walls. This was actually observed in experiments that will be reported in the companion paper [7].

The permanent deformation produced after 80% strain indicates that the cell walls were bent to such an extent that irreversible processes (probably including fracture) occurred in them. It is likely that a permanent deformation is induced whenever cork is deformed in the third, high-slope region of the stress–strain compression curve, when the cell walls cannot bend more due to mutual contacts. This is certainly the situation with a cork stopper, the recovery of which is not complete after being introduced for the first time in a bottle. The strain in this case is biaxial, with $\varepsilon_1 = \varepsilon_2 \simeq 30\%$.

Attempts have been made at fitting the recovery data to simple equations. The simplest equation that describes the recovery of dimensions (both parallel and perpendicular to the direction of compression) with a reasonable accuracy is

$$\varepsilon_r - \varepsilon_{r_\infty} = (\varepsilon_{r_0} - \varepsilon_{r_\infty}) \exp(-kt^\alpha) \qquad (3)$$

where ε_{r_∞} is the strain for $t = \infty$ and ε_{r_0} is the strain at the beginning of recovery (i.e. the strain at the end of compression); k and α are constants, the best values

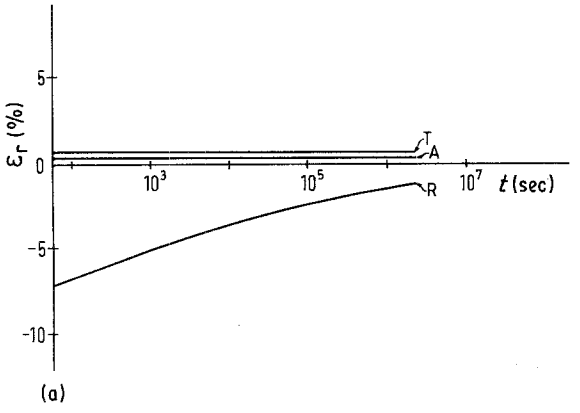

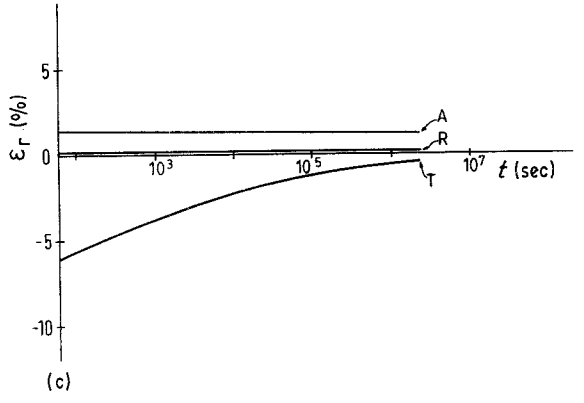

of which are as follows (for t in seconds):

$$k = 0.78 \text{ (SI units)} \qquad \alpha = 0.11$$

For compression strains below ~ 0.75 we may take, in virtue of the previous discussion, $\varepsilon_{r_\infty} = 0$. Above this level, $|\varepsilon_{r_\infty}|$ for the direction of compression can be taken as the excess strain relative to $\varepsilon = 0.75$. For example, for $\varepsilon = 0.8$, we take $|\varepsilon_{r_\infty}| = 0.05$. For the transversal directions, ε_{r_∞} can be taken as zero.

Equation 3 is purely empirical, but may prove useful for practical applications. It does not include a possible effect of the rate of compression on the subsequent recovery, except for the rate effect on the transversal dimensions (i.e. on ε_{r_0}).

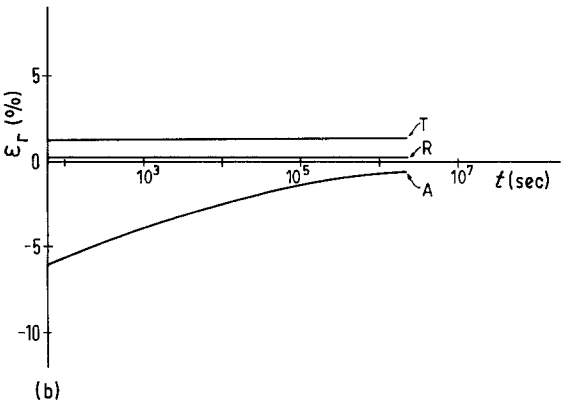

Figure 8 Recovery of dimensions of cork (R = radial dimension, A = axial dimension, T = tangential dimension) following compression up to $\varepsilon = 30\%$ at a strain rate of $2.1 \times 10^{-2}\,\text{sec}^{-1}$. (a) Compression in the radial direction, (b) compression in the axial direction, (c) compression in the tangential direction.

A more complete characterization of viscous effects in cork will be given in the following paper [7], which describes the stress relaxation and creep behaviour of cork.

References

1. L. J. GIBSON, K. E. EASTERLING and M. F. ASHBY, *Proc. R. Soc.* **A377** (1981) 99.
2. M. A. FORTES, *Acta Metall.* **34** (1986) 33.
3. HELENA PEREIRA, M. EMÍLIA ROSA and M. A. FORTES, *IAWA Bull.* **8** (1987) 213.
4. M. F. ASHBY, *Met. Trans.* **14A** (1983) 1755.
5. L. J. GIBSON, M. F. ASHBY, G. S. SCHAJER and C. I. ROBERTSON, *Proc. R. Soc.* **A382** (1982) 25.
6. L. J. GIBSON and M. F. ASHBY, *ibid.* **A382** (1982) 43.
7. M. EMÍLIA ROSA and M. A. FORTES, *J. Mater. Sci.* **23** (1988) 873.

Received 30 March
and accepted 8 June 1987